TOUGHNESS ENHANCEMENT OF AIRFIELD CONCRETE PAVEMENT BY USING SHORT FIBER

Muhammad Mubaraki
Department of Civil Engineering, College of Engineering, Jazan University, Jazan, Saudi Arabia.,
mmubaraki@jazanu.edu.sa

Follow this and additional works at: https://jmstt.ntou.edu.tw/journal

Part of the Engineering Commons

TOUGHNESS ENHANCEMENT OF AIRFIELD CONCRETE PAVEMENT BY USING SHORT FIBER

Acknowledgements

TOUGHNESS ENHANCEMENT OF AIRFIELD CONCRETE PAVEMENT BY USING SHORT FIBER

Muhammad Mubaraki

ABSTRACT

Few efforts have been made to understand the progressive failure of concrete pavements, especially the crack propagation in the concrete materials. More detailed information about concrete material, such as its fracture properties, is required along with the strength to better quantify crack propagation rates of varying concrete mixture proportions and constituents. The susceptibility of concrete pavements to crack growth may be eliminated by adding short steel or glass fibers. Therefore, an experimental study was carried out to investigate the effect of adding short fiber, steel or glass, in controlling the fracture energy of concrete. The analysis was conducted for a constant fiber length of 25 mm. The flexure test of single edge notched as well as unnotched specimens was performed using three-point bending configuration. Four different values of crack-depth ratios were considered, namely 0, 0.1, 0.25, and 0.4. For the same crack-depth ratio, results show that the maximum value of crack mouth opening displacement, and value of curvature in steel-fiber-reinforced concrete (SFRC) were greater than those in glass-fiber-reinforced concrete (GFRC). However, the beam-carrying capacities of GFRC are higher than those of the SFRC for all crack-depth ratios. In general, the fracture energy of the SFRC is greater than that of the GFRC. It is noteworthy that the last portion of moment-curvature curve of the GFRC is steeper than the SFRC curve, thereby indicating that the SFRC is relatively more ductile. The fracture energy depends on the fiber type and crack-depth ratio. Moreover, the fracture energy calculated from notched beam with high crack-depth ratios was found to be more stable and reliable.

I. INTRODUCTION

1. Background

One main challenge that faces engineers of materials is to specify the type and amount of fiber reinforcement for use in concrete pavements. Numerous studies have been carried out to understand the impacts of fiber type and volume fraction on the toughness properties and flexural strengths of the fiber-reinforced concrete. However, there remains a gap in understanding the progressive cracking in concrete pavements and subsequently in understanding the fracture properties. Many theoretical models were proposed to predict the fracture of quasi-brittle materials such as the fictitious crack approach, the two-parameter fracture model, the size effect model, the effective crack model, the cohesive crack model, and the bridged crack model. Testing methods for obtaining the necessary mode I fracture properties to implement these models are reviewed in several text books (e.g. Carpinteri, 1999).

Fibers have been used to reinforce brittle materials. Concrete is one of the main construction materials that is brittle in nature. The concrete like other materials incorporates fibers to enhance composite properties including: tensile strength, compressive strength, elastic modulus, crack resistance, crack control, durability, fatigue life, resistance to impact and abrasion, shrinkage, expansion, thermal characteristics, and fire resistance (ACI Committee 544).

In the late 1950s, use of glass fibers in concrete has been used in Russia. However, it was quickly established that ordinary glass fibers are attacked by the alkali in cement paste, and this finding led to the development of alkali resistant glass fibers. In the early 1960s, evaluation of steel fibers to act as reinforcement for concrete was made in the United States. The use of glass or steel fibers was found to be more effective than the synthetic fibers, such as nylon and polypropylene. As a result, better understanding of the concepts behind fiber reinforcement has led to the conclusion that both synthetic and natural fibers can reinforce plain concrete (ACI Committee 544).

2. Steel Fiber Reinforced Concrete (SFRC)

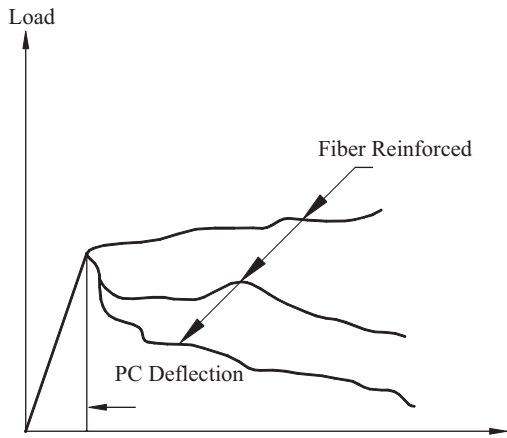Steel fiber reinforced concrete (SFRC) is made up of

Fig. 1. Load versus deflection curves for PC and FRC.

hydraulic cements containing fine aggregate, or both fine and coarse aggregates, and discontinuous discrete steel fibers. In tension, SFRC fails only after the steel fiber breaks or is pulled out of the cement matrix. Properties of fiber include volume percentage, strength, elastic modulus, and fiber bonding parameter of the fibers. Properties of concrete are strength, volume percentage, and elastic modulus. The SFRC is a composite material whose properties can be related to the properties of fiber, concrete, and those of the interface between the fiber and the matrix. These properties play an important role in understanding the mechanics of how the fiber reinforcement strengthens concrete when it extends from the elastic pre-crack state to the partially plastic post-cracked state. A more general and current approach to the mechanics of fiber reinforcement assumes a crack arrest mechanism that is based on fracture mechanics.

Several researchers have achieved encouraging results with different types of fibers. For example, steel fibers improve the ductility of concrete under all modes of loading, but their effectiveness in improving strength varies among compression, tension, shear, torsion, and flexure., In compression, the ultimate strength is only slightly affected by the presence of fibers, with observed increases ranging from 0 to 15 percent and up to 1.5 percent by volume of fibers (ACI Committee 544). Recently Cagginao et al. (2012) found that adding 0.05% of steel fiber decreased the compressive strength of concrete while adding 0.1% of steel fiber increased the compressive strength of concrete. On the other hand, Kabay (2014) found that the addition of basalt fibers decreased the compressive strength of concrete. Studies in tension showed that the improvement in strength is significant. Increases of the order of 30 to 40 percent were reported for the addition of 1.5 percent by volume of fibers in mortar or concrete. Furthermore, steel fibers generally increase the shear and torsional strength of concrete, although there is little data dealing strictly with the shear and torsional strength of the SFRC, as opposed to that of reinforced beams made with an SFRC matrix and conventional reinforcing bars. Fig. 1 shows typical load-deflection curves

for plain concrete and fiber reinforced concrete beams under flexure. It is evident from the results of various studies that the addition of fiber increased the flexural toughness significantly.

Kabay (2014) studied the effects of basalt fiber addition in high strength and normal strength concrete with different water to cement ratios. The author found that the addition of basalt fiber could provide significant contributions to concretes in terms of flexural strength, fracture energy and abrasion resistance. Koksal et al. (2013) concluded that the performance of fiber reinforced concrete depends much on the properties of steel fibers in concrete, when the matrix strength is high. Thus, congruence between matrix and steel fiber strengths is required and it must be taken into consideration when designing steel fiber reinforced concrete mixes in order to maximize the fracture energy and minimize the cost of the mix. Karihaloo et al. (2013) found that the specific fracture energy G_f measured is highly dependent on the size of the specimen and the notch to depth ratio. Ren and Li (2013) developed a numerical model to simulate the behavior of fiber reinforced concrete in meso-level. They concluded that the proposed damage model could include the tensile as well as the compressive damages in a unified framework. Based on the existing numerical methods, the compressive behaviors of the FRC in theme so scale are neither well understood nor precisely simulated.

3. Glass Fiber Reinforced Concrete (GFRC)

The GFRC is made of cement, AR-glass fibers, sand, and water. It is a non-combustible material and meets the criteria of ASTM E136. When used as a surface material, its flame spread index is zero (PCI Committee, 1993). The GFRC which is made with acrylic thermoplastic copolymer dispersion for curing purposes will not pass ASTM E136 criteria, but will have a flame spread index of less than 25. Mechanical properties of the GFRC composites depend upon fiber content, polymer content (if used), water-cement ratio, porosity, sand content, fiber orientation, fiber length, and curing (PCI Committee, 1993). The primary properties of spray-up GFRC used for design are the 28-day flexural Proportional Elastic Limit (PEL) and the 28-day flexural Modulus of Rupture (MOR) (PCI Committee, 1993). The PEL stress is a measure of the matrix cracking stress. The 28-day PEL is used in design as the limiting stress to ensure that the longterm in-service panel stresses are maintained below the composite cracking strength. In addition, de-molding and other handling stresses should remain below that of the material at the specific time of the event. A generalized load-deflection curve for a 28-day GFRC composite subjected to a flexure test showed that GFRC composites typically possess considerable load and strain capacity beyond the matrix cracking strength. The mechanism that is primarily responsible for this additional strength and ductility is fiber pullout. Upon first cracking, much of the deformation is attributed to fiber extension. As load and deformation continue to increase, and multiple cracking occurs beyond the proportional elastic limit, fibers begin to debond and subsequently slip or pull out to span the cracks and resist the applied

load. Load resistance is developed through friction between the glass fibers and the cement matrix as the fibers debond and pull out (PCI Committee, 1993).

4. Rigid Pavement and Its Types

A rigid pavement structure is composed of a Portland Cement Concrete (PCC) surface course built on the top of the subgrade or base course. The surface course provides characteristics such as friction, smoothness, noise control and drainage. The base course consists of aggregate or stabilized subgrade. It provides additional load distribution and drainage. Sometimes subbase course is used and it is the portion of the pavement structure between the base course and the subgrade. Its main function is to provide structural support.

During the construction, the joints are required to be placed in a rigid pavement surface course. The types of the pavement joints are contraction, expansion, isolation, and construction. A contraction joint in a concrete slab creates a weakened vertical plane. It regulates the location of the cracking caused by dimensional changes in the slab. An expansion joint is placed at a specific location to allow the pavement to expand without damaging adjacent structures or the pavement itself. However, expansion joints are not typically used because their progressive closure tends to cause contraction joints to progressively open (Abdel-Maksoud et al., 1997). An isolation joint is used to lessen compressive stresses that develop at unsymmetrical and T-intersections, manholes, drainage inlets, and at places where movement between the pavement and a structure may take place (FHA, 1990). They are typically filled with a joint material to prevent water and dirt infiltration. A construction joint is a joint between slabs that results when concrete is placed at different times. This type can be broken into transverse and longitudinal construction joints.

Since all rigid pavements are made with Portland Cement Concrete (PCC) therefore, this paper aims to investigate the fracture resistance to crack growth. The author prefers to classify the rigid pavements into three major categories by their means of crack control:

- Jointed Plain Concrete Pavement (JPCP)
- Jointed Reinforced Concrete Pavement (JRCP)
- Continuously Reinforced Concrete Pavement (CRCP)

1) Jointed Plain Concrete Pavement (JPCP)

This type is common in rigid pavement. JPCP controls cracks by dividing the pavement into individual slabs separated by contraction joints. JPCP does not use any reinforcing steel. However, it uses dowel bars and tie bars.

2) Jointed Reinforced Concrete Pavement (JRCP)

JRCP controls cracks by dividing the pavement into individual slabs separated by contraction joints. JRCP uses reinforcing steel within each slab to control within-slab cracking. Due to some longterm performance problems, JRCP is no longer in use in many countries across the world.

3) Continuously Reinforced Concrete Pavement (CRCP)

CRCP uses reinforcing steel rather than contraction joints for crack control. Cracks are held tightly together by the underlying reinforcing steel.

4) Cracking Mechanism and Load Transfer

Jointed plain concrete pavement (JPCP) uses contraction joints to control cracking and does not use any reinforcing steel. Transverse joint spacing is selected so that temperature and moisture stresses do not produce intermediate cracking between the joints. Dowel bars are typically used at transverse joints to assist in load transfer and the tie bars are typically used at longitudinal joints. The crack is controlled by contraction joints, both transverse and longitudinal. The joint spacing for the contraction joint is recommended to be between 3.7 meter and 6.1 meter as the slabs will crack in the middle if it is more than 6.1 meter. When a wheel load is applied at a joint or crack, both the loaded slab and the adjacent unloaded slab deflect. The amount of deflection in the unloaded slab is directly related to joint performance. For example, if a joint is performing perfectly, then both the loaded and unloaded slabs deflect equally. Therefore, the load transfer mechanism depends on temperature that affects joint opening, joint spacing, and aggregate particle angularity (Martin-Perez and Pantazopoulou, 2001). Most performance problems with concrete pavement are a result of poorly performing joints. The poor load transfer creates high slab stresses, which contribute heavily to distresses. Thus, adequate load transfer is vital to rigid pavement performance. Load transfer across transverse joints is accomplished using aggregate interlock, dowel bars, or reinforcing steel.

II. PROBLEM STATEMENT

The increase in repetitive aircraft loading on concrete pavements and the variation in available concrete material constituents pose challenges in the structural design of concrete pavements and prediction of slab's performance throughout its service life. The failure of concrete around dowel bars in jointed rigid pavements and the resulting effect on the performance can be improved by adding fibers to the concrete matrix. Inserting steel fibers or glass fibers with certain volume fraction in the concrete matrix proved to be beneficial on the toughness properties and flexural strengths resulting in reduced distress at pavement discontinuity such as corner cracking and joint faulting (Fu and Lauk, 1996).

As a composite, the overall material properties change. This change is based on the interaction and the volume ratio of the fiber relative to the matrix. The major properties of FRC are: increased tensile strength, increased toughness, reduced crack widths, crack propagation rates, reduced shrinkage, increased fatigue resistance, impact resistance, increased post-cracking ductility, and lower rheological properties (Balaguru and Shah, 1992). The fiber material is chosen to be one with greater composite flexural strength or increased ductility rela-

tive to concrete. The fibers are used for the purpose of improving the durability of the element due to their effectiveness with regard to cracking control at early ages and in the hardened state (Pujadas et al., 2012).

III. METHODOLOGY

1. Experimental Work

In the present experimental program, we used several tests to determine the fracture energy of steel and glass fibers reinforced concrete in the presence of silica fume. It was a three-point bending test of notched, with three different values of crack to depth ratios (a/d), namely 0.1, 0.25 and 0.4, and unnotched specimens. The silica fume content was equal to 10% and the steel or glass fiber volume fraction was equal to 1%. The length of the fiber was kept constant at 25 mm during the experiments. The dimensions of the flexural and fracture toughness test specimens were $100 \times 100 \times 350$ mm with a loaded span of 300 mm.

2. Materials

Type I ordinary Portland cement was used as binding material. The cement content for the control mix was 450 Kg/m^3. Ordinary siliceous sand with a fineness modulus of 2.7, bulk density of 1700 Kg/m^3 and specific gravity of 2.45 was used as fine aggregate. Coarse aggregate (natural gravel) with a maximum size of 14 mm, bulk density of 1650 Kg/m^3 and specific gravity of 2.66 was used. Light gray silica fume of specific surface area of 18 m^2/gm was used. Plain mild steel and high zirconia alkali resistance glass (NEG ARG) fibers were used in this investigation. In the case of steel fiber, the fiber aspect ratio was 50, and the modulus of elasticity and the yield strength were 200 GPa and 265 MPa, respectively. For the glass fiber, it was supplied in chopped strands of 25 mm long. The modulus of elasticity and the ultimate tensile strength were 74 GPa and 1.4 GPa, respectively. The mix proportion (cement: sand: gravel: water/cementitious materials ratio) by weight for the control mix was 1: 1.6: 2.25: 0.35. Due to the relatively low water content and the presence of silica fume and fibers, a super plasticizer was added to the mixing water in order to improve the workability and to keep the slump as constant as possible. It is very important to note that the fibers should be dispersed uniformly throughout the mixture. This must be done during the batching and mixing phase. The fibers are added to the mixer after all other ingredients, including the water have been added and mixed. Fibers are then added manually into the mix as recommended by ACI Committee 544 (ACI Committee 544). Therefore, the recommended mixing sequences were adopted in the present work for all the mixes.

3. Test Specimens and Procedure

The bending and fracture toughness test specimens were cast in wooden molds. The molds were coated by a thin layer of oil before casting. A steel plate of 0.8 mm thickness was used to create the notch at the tensile surface of the fracture toughness test specimens. A universal hydraulic testing machine of 1000 kN maximum capacity was used for testing all the specimens after 28 days. A dial indicator of a mechanical type having an accuracy of 0.01 mm was used to measure the crack mouth opening displacement (CMOD).

IV. RESULTS AND DISCUSSION

The effect of silica fume content and steel fiber volume fraction on the mechanical properties (compressive, indirect tensile and flexural strengths) of fiber reinforced concrete (FRC) was previously studied by the author (Sallam and Mubaraki, 2013). Three ratios of silica fume content as partial replacement by cement weight, i.e. 5, 10, and 15% and two volume fractions of steel fiber, 0.5, and 1%, were considered in the previous study. The experimental results showed that there is an increase in the indirect tensile and flexural strengths, while there is a decrease in the compressive strength with the addition of steel fiber. These results agreed with the results obtained by Kabay (2014) for basalt fiber reinforced concrete. They also support the findings obtained by Caggiano et al. (2012) for steel fiber reinforced concrete with fiber volume fraction equals 0.05%. On the other hand, at the same fiber volume fraction, all strengths increased proportionally by increasing the silica fume content. The presence of fibers reduces the degree of brittleness of concrete, hence, changes the mode of failure from the state of being brittle to be more ductile.

Fig. 2 shows the stress-CMOD behavior of steel and glass FRC for different initial crack lengths. It clearly shows the numbers of significant conclusions. The CMOD at the maximum Stress, σ_{max} increased with increasing a/d ratio. For the same fiber volume fraction and a/d ratio, σ_{max} of glass FRC is higher than that of steel fiber because the ultimate strength of glass fiber is higher than that of steel fiber. Although the maximum value of CMOD, at any value of a/d, in the case of steel fiber was greater than that of the glass fiber. The CMOD at σ_{max} exhibited an opposite trend. This may be attributed to the difference in the bond between the fibers and the concrete and the maximum deformation of the two fibers. It was observed that the steel FRC has greater resistance to load than the glass FRC in the descending part of the curve. This could be due to the fact that steel is a ductile material and glass is a brittle material. It should be noted that Nelson et al. (2002) divided the σ-CMOD curve in five zones; three in the ascending part and two in the descending part. Zone I is characterized by linear elastic behavior. Zone II contains the nonlinear deformation of the composite resulting from the micro-crack formation. In Zone III, the localized failure crack is formed and is growing in a stable manner. Zone IV contains the unstable growth of the localized failure crack. Finally, in Zone V, the failure crack has propagated across the entire specimen's depth, and only the bridging fibers carry the load. They were found in the case of polypropylene fiber that Zone
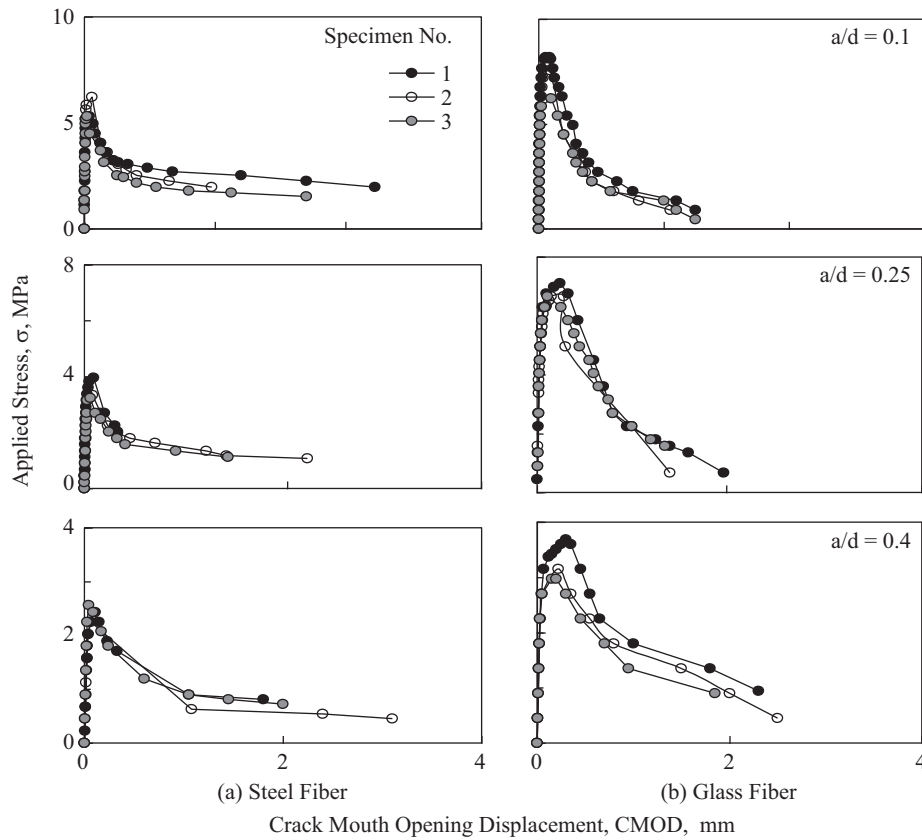
Fig. 2. Stress-crack mouth opening displacement curves for different crack length (a) steel fiber and (b) glass fiber.

II was very narrow (Nelson et al., 2002). They attributed this observation to the inability of fiber to stabilize the micro-crack formation prior to the development of the localized failure. On the other hand, the results of this study show that the size of Zone II and Zone III is small. Therefore, it can be ignored for simplicity. The size of Zones II and III may depend on the fiber volume fraction, the fiber geometry, and the bond strength between fiber and concrete. Therefore, trilinear σ-CMOD curve can explain the deformation in FRC.

The fracture energy was calculated according to the RILEM Committee 50-FMC (RILEM, 1985) for plain concrete. The fracture energy, G_F, was drawn against the crack-depth ratio in Fig. 3 for glass and steel FRC. The fracture energy is affected by the a/d ratio. The smallest fracture energy and size may be achieved at high a/d ratios. Therefore, the present results support the recommendations of the RILEM with a/d = 0.5. Furthermore, Lee and Barr (2003) concluded that the notched beam is a better geometry than the unnotched beam mainly in terms of test stability and reliability. Karihaloo et al. (2013) concluded that the specific fracture energy, G_F measured using the RILEM work-of-fracture procedure is highly dependent on the size of the specimen and the notch to depth ratio. For all values of a/d, the fracture energy of steel fiber reinforced concrete is higher than that of glass fiber reinforced concrete. This means that the fiber with a higher modulus of elasticity and ductility (steel fiber) is more efficient than the fiber of
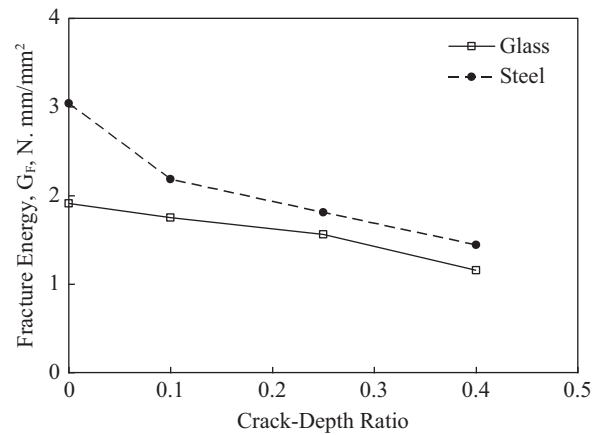

Fig. 3. Fracture energy of glass and steel FRC.

higher strength (glass fiber). On the other contrary, Koksol et al. (2013) found that the steel fibers with a low tensile strength exhibit a good performance, resulting in high fracture energy values, for low matrix strengths. However, steel fibers with a high tensile strength are more effective for high matrix strength in point of fracture energy.

Fig. 4 shows the Moment-Curvature behavior of steel and glass FRC for unnotched and notched specimens. For the same a/d ratio, the maximum curvature in the case of steel
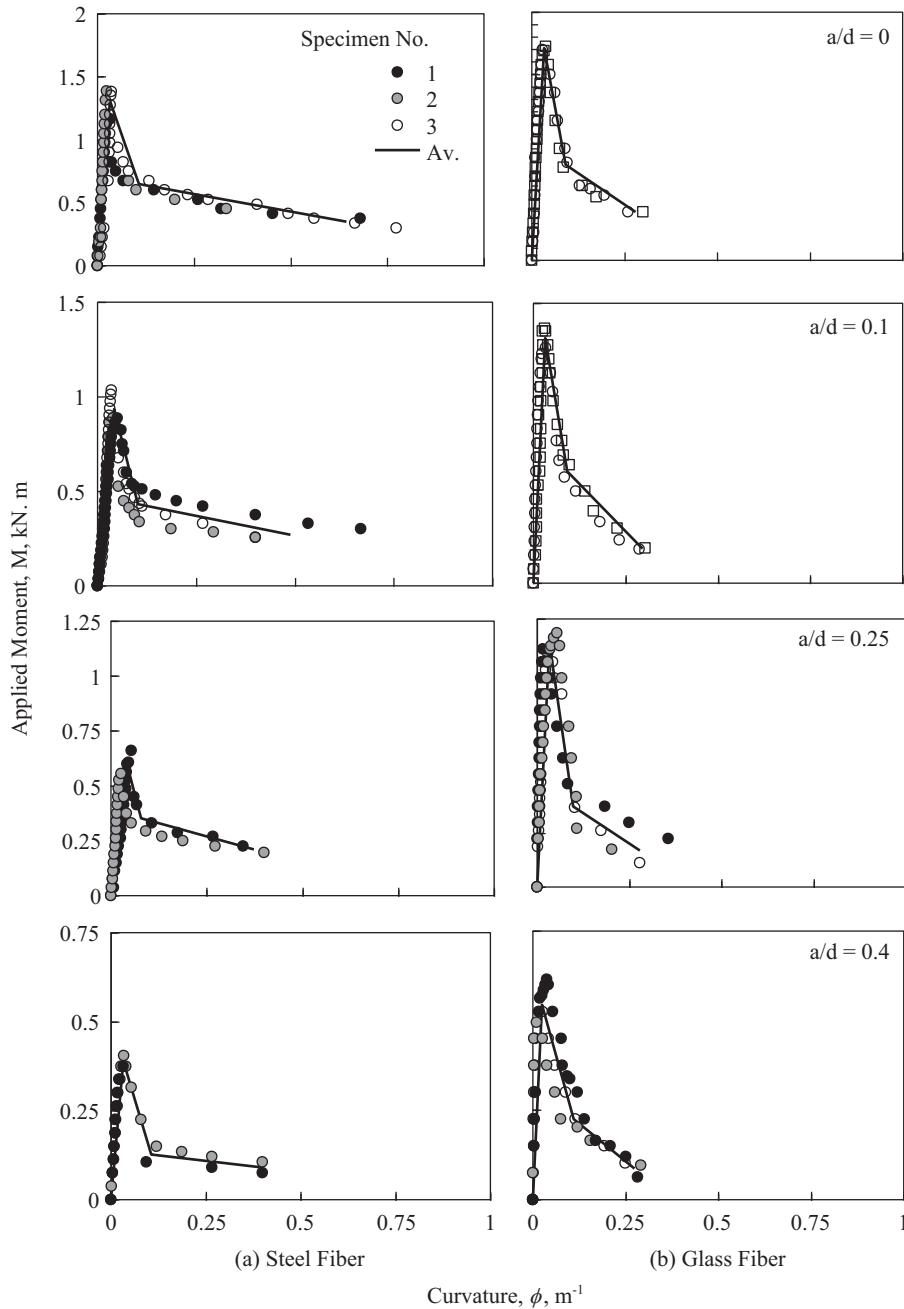
Fig. 4. Moment-Curvature curves for notched and unnotched specimens (a) steel fiber and (b) glass fiber.

fiber was greater than that of the glass fiber, while the curvature at the maximum moment exhibited an opposite trend. The average value of each of the three specimens was calculated to get a simple trilinear M-ϕ curve for FRC as shown in the figure. This means that the first three deformation zones which were suggested by Nelson et al. (2002) were merged as one zone. Fibers along the fracture plane prevent the crack from opening and delay the propagation of the crack. The tension softening diagram (the part of M-ϕ curve after peak Moment) can describe the post-cracking behavior and express the resistance of concrete against crack development

(Koksal, 2013).

V. CONCLUSIONS

Based on the experimental results, the following conclusions were made:

- For the same crack-depth ratio, the maximum value of CMOD and curvature in the case of steel fiber were greater than those of the glass fiber.
- The strengths of glass fiber reinforced concrete measured

from notched and smooth beams under flexural are higher than those of steel fiber reinforced concrete.

- The last portion of moment-curvature curve of GFRC is much steeper than the SFRC curve, indicating that the SFRC is more ductile.
- Steel fiber reinforced concrete has a higher fracture energy than that of the glass fiber reinforced concrete for all values of crack length to beam depth ratio.
- The fracture energy calculated from notched beam with high values of a/d ratio was found to be more stable and reliable.

ACKNOWLEDGMENTS

REFERENCES

Abdel-Maksoud, M., G. N. Hawkins and E. Barenber (1997). Behavior of concrete joints under cyclic shear. ASCE Conference on Aircraft Pavement Technology, Seattle, Washington.

ACI Committee 544 (2002). State of the Art Report on Fiber Reinforced Concrete, ACI Committee 544. 1R-96.

Balaguru, P. N. and S. P. Shah (1992). Fiber Reinforcement Cement Composites. McGraw-Hill: New York, NY.

Caggiano A., M. Cremona, C. Faella, C. Lima and E. Martinelli (2012). Fracture behavior of concrete beams reinforced with mixed long/short steel fibers. Construction and Building Materials 37, 832-840.

Carpinteri, A. E. (1999). Nonlinear crack models for nonmetallic materials. Kluwer Acad. Pub., Dordercht.

Federal Highway Administration (1990). Concrete Pavement Joints. Technical Advisory T 5040.30 Federal Highway Administration, Washington, D.C.

Fu, S.-Y. and B. Lauk (1996). Effects of fiber length and fiber orientation distributions on the tensile strength of short-fiber- reinforced polymers. Composites Science and Technology 56, 635-652.

Kabay, N. (2014). Abrasion resistance and fracture energy of concretes with basalt fiber. Construction and Building Materials 50, 95-101.

Karihaloo, B. L., A. R. Murthy and N. R. Iyer (2013). Determination of size-independent specific fracture energy of concrete mixes by the tri-linear model, Cement and Concrete Research. 49, 82-88.

Koksal, F., Y. Sahinb, O. Gencel and I. Yigit (2013). Fracture energy-based optimization of steel fiber reinforced concretes. Engineering Fracture Mechanics 107, 29-37.

Lee, M. K. and B. I. G. Barr (2003). Strength and fracture properties of industrially prepared steel fiber reinforced concrete. Cement & Concrete Composites 25, 321-332.

Martin-Perez, B. and S. J. Pantazopoulou (2001). Effect of bond, aggregate interlock and dowel action on the shear strength degradation of reinforced concrete. Engineering Structure 23, 214-227.

Nelson, P. K., V. Li and T. Kamada (2002). Fracture toughness of microfiber reinforced cement composites. Journal of Materials in Civil Engineering 14, 384-391.

PCI Committee on Glass Fiber Reinforced Concrete Panels (1993). Recommended Practice for Glass Fiber Reinforced Concrete Panels. Pre-cast/ Prestressed Concrete Institute, Chicago.

Pujadas, P., A. Blanco, A. de la Fuente and A. Agnado (2012). Cracking behavior of FRC slabs with traditional reinforcement. Material and Structures 45, 707-725.

Ren, X. and J. Li (2013). Multi-scale based fracture and damage analysis of steel fiber reinforced concrete. Engineering Failure Analysis 35, 253-261.

RILEM Committee on Fracture Mechanics of Concrete-Test Methods (1985). Determination of the fracture energy of mortar and concrete by means of three-point bend test on notched beams. Materials and Structures 18, 285-290.

Sallam, H. E. M. and M. Mubaraki (2013). Fracture energy of fiber reinforced concrete for rigid pavements. Proceeding of 17th IRF World Meeting & Exhibition, International Road Federation (IRF), Riyadh, Saudi Arabia.